ISSN NO: 9726-001X
Volume 11 Issue 03 2023

JOURNAL OF CURRENT SCIENCE

THE USE OF DIGITAL IMAGE CORRELATION FOR STRAIN DISTRIBUTION MEASUREMENT IN TENSILE TESTS ON METALS, WITH STRESS-STRAIN RELATIONSHIP TAKEN INTO ACCOUNT

Dr.Naveen.R, Dr. K.G.Prakash, Chandrakumar.C

Asst. Professor, Asst. Professor, Asst. Professor

shivaganesh.ng@gmail.com, prakashkg059@gmail.com, chakrapdit@gmail.com

Department of Mechanical, Proudhadevaraya Institute of Technology, Abheraj Baldota Rd, Indiranagar, Hosapete, Karnataka-583225

Abstract

The digital image correlation approach was used to assess the displacement distribution in the aluminium plate specimen during the tensile test. The strain distribution was then calculated from this displacement distribution. During the complete tensile test, we were able to measure the change in strain distribution. Although strain in other areas of the material essentially remains constant, localised strain becomes more pronounced as deformation progresses and appears before proof stress. The stress-strain relationship states that when real strain increases, the true stress, which is determined from the conventional average stress in the specimen's uniform area, drops after proof stress. As the real strain rises, the true stress calculated from the specimen's maximum strain also increases, indicating the presence of work hardening. A comparison was made between the stress-strain relationship for aluminium and the previously reported finding for steel. In order to assess the stress-strain relationship precisely, it is necessary to quantify the distribution of strain and take into account the local maximum strain.

Key words: Experimental mechanics, Displacement measurement, Digital image correlation, Local deformation, Stress-strain relation

1. Introduction

In tensile test of metallic materials, measurement of distance between two gage marks on a specimen is regulated as a parameter to express elongation of the specimen in JIS (Japanese Industrial Standards Committee, 2011). Average strain in gage length can be obtained from change of gage length based on measurement of the conventional tensile test. Average strain is reasonable as a parameter to express the surface strain on the specimen in the case of uniform deformation. For the case of non-uniform deformation, magnitude of strain is not uniform on specimen surface and average strain may not be adequate to express the strain appeared actually on the specimen. For consideration of stress-strain relation based on the average strain may not always be reasonable in this case.

In the previous paper, the author investigated about measurement of strain distribution continuously on specimen surface during tensile test of steels using digital image correlation (DIC) method (Kato, 2015). Change in strain distribution on specimen surface in yielding stage was measured and generation and spread of Lüder's band were observed by measuring the plastic strain quantitatively. Local strain in the necking area was measured in the later stage of the test after maximum load and change in the maximum strain was observed until just before the fracture. Evaluation of stress-strain relation is important to derive parameters for materials characteristics and has been investigated for steels by many researchers so far (Tuchida, 2014). In our previous study, stress-strain relation was considered based on the local maximum strain instead of the conventional average strain in uniform area of the specimen and we could get a linear relationship until just before fracture similar to the relationship in the uniform plastic deformation stage before maximum loading.

In this paper, the author measured strain distribution of specimen surface for plate specimens of aluminum during tensile test and observed occurrence of non-uniform strain distribution appeared during the test and compared for the

ISSN NO: 9726-001X
Volume 11 Issue 03 2023

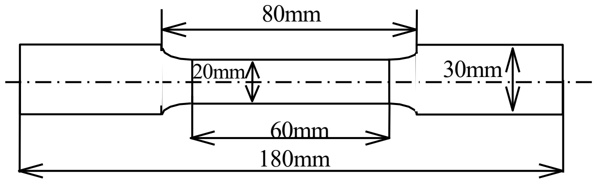

t=3mm Fig. 1 Test specimen

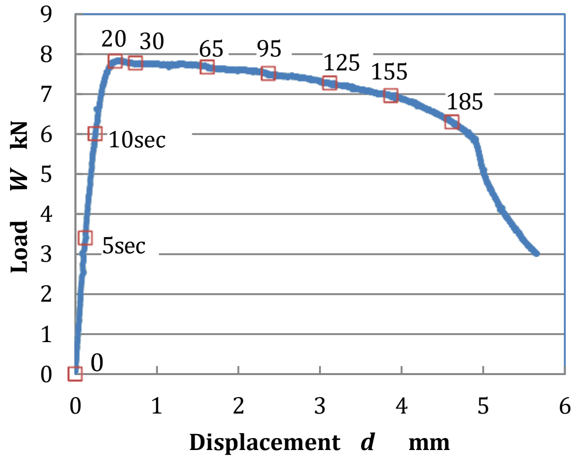

Fig. 2 Load-displacement curve for A1050 (Numbers in the graph show elapsed time (sec) from start of the test)

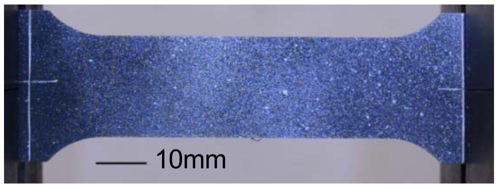

(a) 0 sec

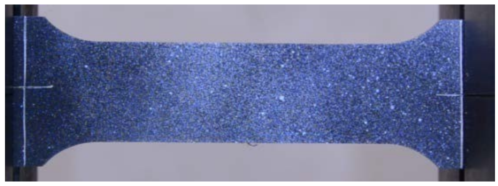

(b) 30 sec

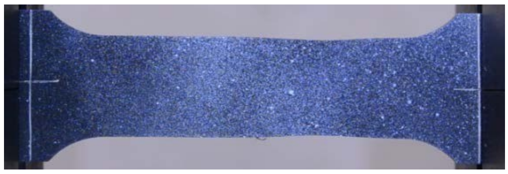

(c) 95 sec

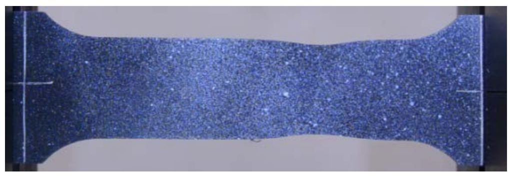

(d) 155 sec

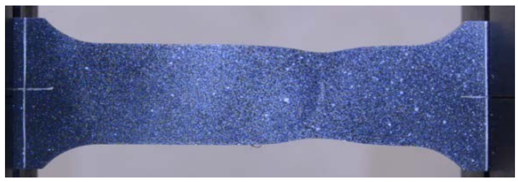

(e) 185 sec

Fig. 3 Images of specimen surface during tensile test

case of steels. In the transition stage from elastic to plastic deformation, strain distribution change around proof stress for aluminum was observed and compared to the yielding for steels. Strain distributions were measured during whole tensile test and stress-strain relation was considered until just before fracture. In consideration of stress-strain relation, obtained result based on local strain was compared to the conventional average strain in uniform sectional area of the specimen and necessity of considering local maximum strain for stress-strain relation is discussed in this paper.

2. Experimental Procedure

Material used in this study is aluminum A1050 in JIS. Test specimen is a plate specimen as shown in Fig. 1. Thickness of the specimen is 3mm. Tensile test was made under a constant tensile speed with about 2mm/min. Load and displacement signals were taken into PC through A/D converter board from the test machine. White paint was sprayed and small random dots were made on the specimen surface after black paint was sprayed on the whole measurement area on the specimen. Image of the surface of a specimen was taken continuously without stopping the test machine as a movie during whole tensile test with a digital camera (NIKON D5500 with a lens of f=55mm). The camera was set in front of the specimen 400 mm apart from the surface. Time on the PC monitor was taken in a movie with the digital camera before the test and time of the PC was corresponded to the time of the movie. The movie file taken during the test was converted to static images with each one second after the test

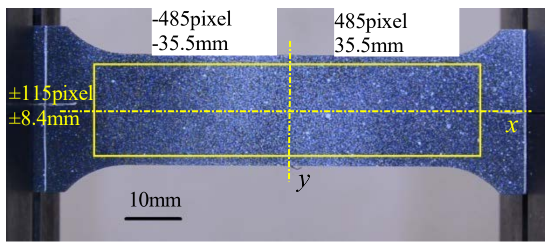

Fig. 4 Measurement area

JOURNAL OF CURRENT SCIENCE

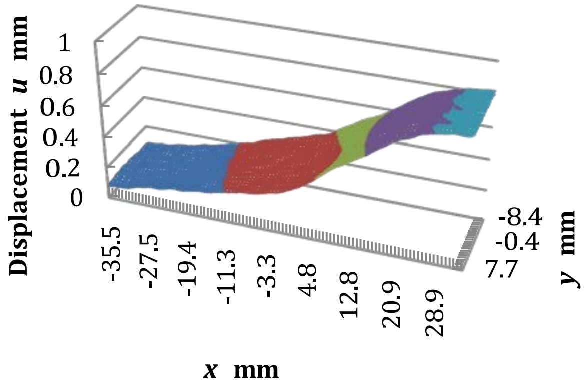

(a) Displacement *u*

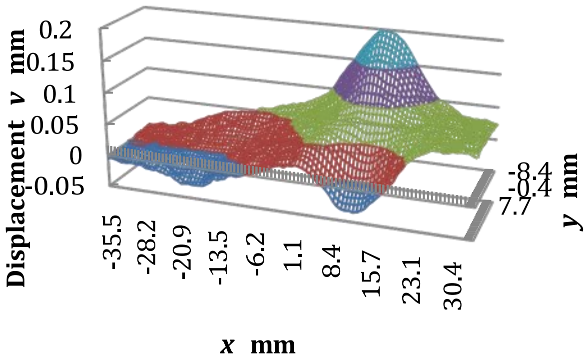

(b) Displacement *v*

Fig. 5 Displacement distributions (at 35 sec)

and images were selected from those static images for the analysis of DIC method.

Load-displacement curve for the tensile test is shown in Fig. 2. Numbers in the graph show the elapsed time (sec) from start of the test and the position where strain distribution was measured in this paper. Load increases linearly with displacement in the earlier stage and then the load takes the maximum value and then the load decreases gradually after taking the maximum value. Decrease rate of the load becomes larger with increase of the displacement and then the specimen fractures finally. This tendency of load-displacement curve is similar to the result previously published by the other researchers (Tokuda et al, 2014) (Noguchi, 2013)

Images of the specimen surface during the test are shown in Fig. 3 for each time shown in the load-displacement curve in Fig. 2. Displacement distribution was measured for each image of specimen surface from the initial image with the load of almost 0 N shown as 0 sec in the picture using DIC method. Area where displacement distribution was measured is shown with the rectangle in Fig. 4. Displacement was measured with each 10-pixel step on *x* and *y* direction within the area. About DIC method for displacement measurement, many literatures have been published (W.F. Chu et al, 1985) and the details are not explained in this paper. About the basic parameters used in this study, subset size for the window for DIC was 31x31 pixels. Window for the subset is deformed by bi-linear function for *x* and *y* direction and interpolation of gray level between adjacent pixels is made with linear equation in DIC calculation.

3. Measurement of Strain Distribution

Figure 5 shows displacement distribution *u* and *v* measured for the image at 35 sec for A1050. From displacement distribution, we calculated strain distribution. We considered a window with adjacent 7x7 measured points of *u* and *v* for

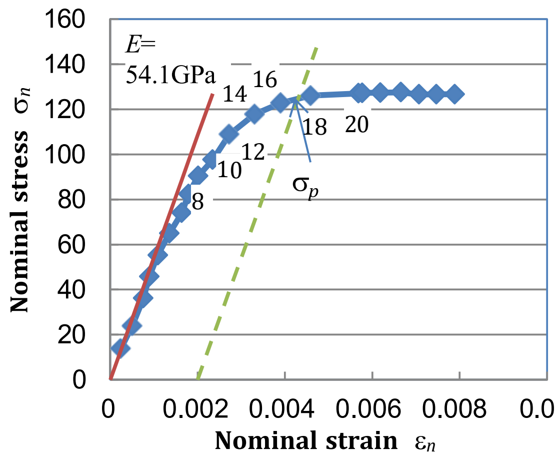

Fig. 6 Nominal stress-strain curve (from elastic to transition stage)

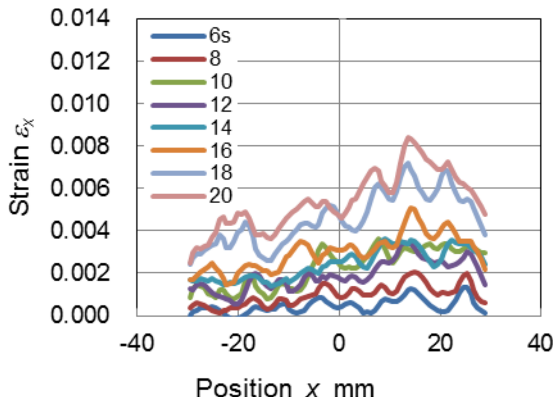

Fig. 7 Distribution of strain (in transition stage from elastic to plastic deformation)

ISSN NO: 9726-001X
Volume 11 Issue 03 2023

calculation of strain components. Coordinates x_c and y_c was considered with the origin at the center of this calculation window. Distribution of measured u and v were approximated with second-order polynomials for x_c and y_c as the following equations.

$$u = a_0 + a_1 x_c + a_2 y_c + a_3 x_c y_c + a_4 x_c^2 + a_5 y_c^2 \quad (1)$$
$$v = b_0 + b_1 x_c + b_2 y_c + b_3 x_c y_c + b_4 x_c^2 + b_5 y_c^2 \quad (2)$$

The coefficients in the equations can be obtained from the measured displacements at 7x7 points. Strain components ε_x, ε_y and γ_{xy} can be obtained with the following equations.

$$\varepsilon\varepsilon_x = \frac{\partial u}{\partial x_c} = a_1 + a_3 y_c + 2a_4 x_c \quad (3)$$
$$\varepsilon\varepsilon_y = \frac{\partial v}{\partial y_c} = b_2 + b_3 x_c + 2b_5 y_c \quad (4)$$
$$\gamma\gamma_{xy} = \frac{\partial u}{\partial y_c} + \frac{\partial v}{\partial x_c} = a_2 + a_3 x_c + 2a_5 y_c + b_1 + a_3 y_c + 2b_4 x_c \quad (5)$$

At the center position (x_c=0, y_c=0), the strain components are given with the following equations.

$$\varepsilon\varepsilon_x = a_1,\ \varepsilon\varepsilon_y = b_2,\ \gamma\gamma_{xy} = a_2 + b_1 \quad (6)$$

Strain distribution for the whole measured area was calculated with moving the window of 7x7 measured points.

Figure 6 shows relation between nominal stress and strain obtained from the experiment in this study. The figure shows stress-strain relation in the stage from elastic deformation to around proof stress. The nominal stress in this graph is obtained from load W divided by the initial sectional area A_0 and the nominal strain is the conventional average strain in uniform area of the specimen. In the earlier stage of elastic deformation, stress-strain relation is almost linear and Young's modulus is estimated as 54.1 GPa from the gradient. From the value of Young's modulus, proof stress with 0.2% plastic strain can be estimated as about 125 MPa shown in the figure and is located between 16sec and

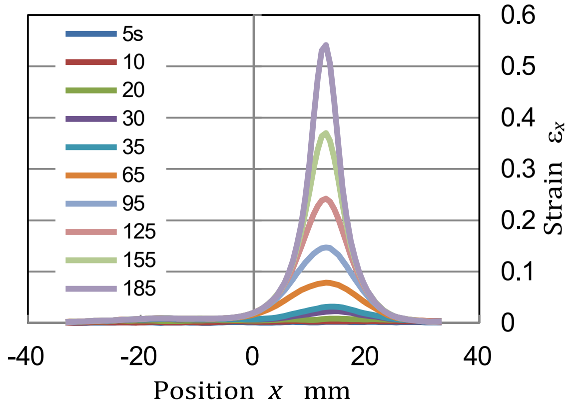

(a) on x-direction

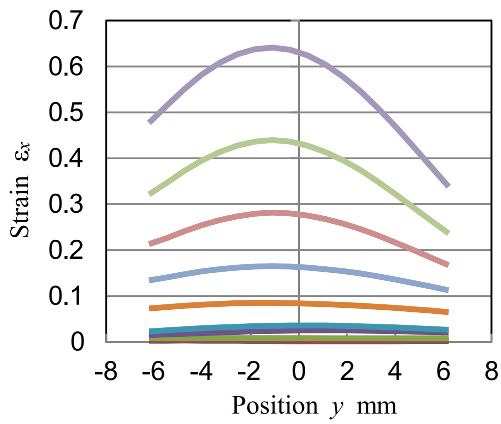

(b) on y-direction

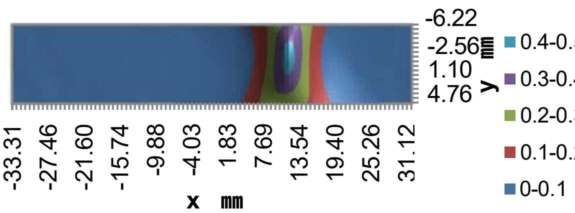

(c) Strain distribution at t=155sec

Fig. 9 Distribution of strain ε_x

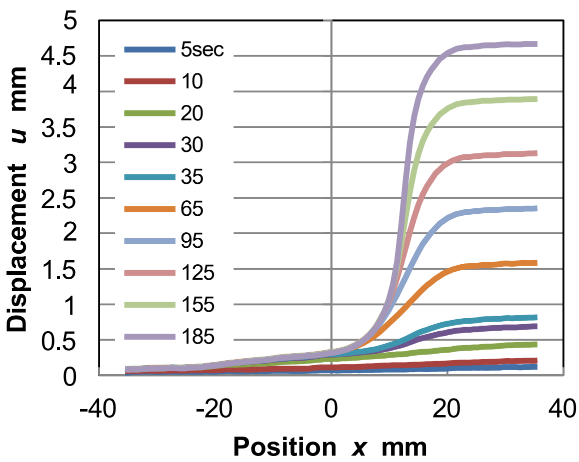

Fig. 8 Distribution of displacement u on x-direction

ISSN NO: 9726-001X
Volume 11 Issue 03 2023

18sec in stress-strain curve.

Change in strain distribution was investigated around proof stress. Figure 7 shows distribution of strain ε_x on x-direction at the center y=0 at the time shown in the figure. In elastic deformation stage, strain distribution has a scatter in distribution but it is almost uniform from 8sec to 14sec. Strain distribution is not uniform and large strain is seen clearly at a position of x with about 15mm at 16sec in the stage before proof stress. Thus non uniform distribution of plastic strain seems to appear and concentrated large strain exists before proof stress. And the concentrated strain becomes larger for later time of the test.

Figure 8 shows distribution of displacement u on x-direction at specimen axis at the time shown in the figure. In elastic deformation stage, displacement distribution is linear to the position x. However, the displacement distribution changes largely after elastic deformation stage and the change becomes more drastically for progress of the tensile test.

Distribution of strain ε_x obtained from the displacement distribution is shown in Fig. 9 (a) on x-direction at y=0. Non uniform distribution starts around proof stress and large strain appears around x= 15mm. The maximum strain increases with progress of tensile test. Strain distribution on y-direction at the position of x with maximum strain is shown in Fig. 9 (b). Strain distribution around maximum strain is not uniform on the vertical direction to the specimen axis and strain is larger at the center and decreases to the edge of the specimen. Example of strain distribution of the specimen surface at the time 155 sec is shown in Fig. 9 (c).

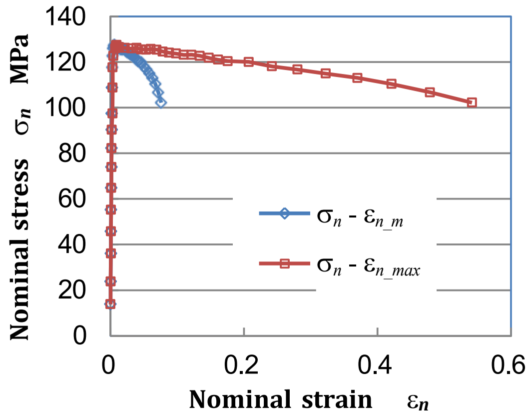

(a) Nominal stress-strain

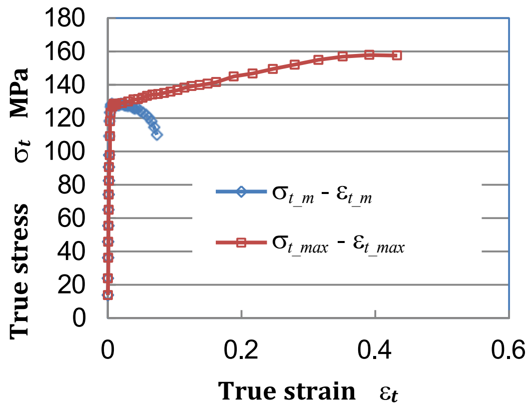

(b) True stress-strain

Fig. 10 Stress-strain relations

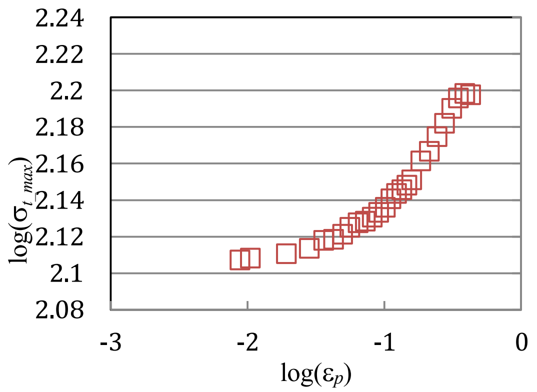

(a) $\sigma_{t\ max}$ vs. ε_p

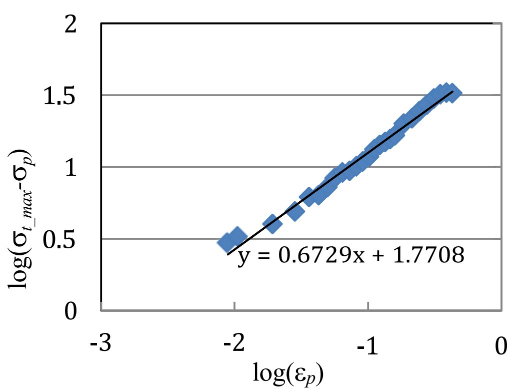

(b) $\sigma_{t\ max}$ -σ_p vs. ε_p

Fig. 11 Relation between $\sigma_{t\ max}$ and ε_p

4. Relation between Stress and Strain

In Fig. 10(a), relation between nominal stress and nominal strain is shown. In the graph, nominal stress σ_n is defined as load W divided by the initial cross sectional area of the specimen, A_0. For nominal strain, two kinds of definition were considered. The one ε_{n_m} is average value of strain ε_x in the uniform area of the specimen and is the conventional nominal strain. The other ε_{n_max} is the maximum strain shown in Fig. 9 (a) with averaging on y-direction shown in Fig. 9 (b). Relations between σ_n and ε_{n_m} and also σ_n and ε_{n_max} are shown in Fig. 10 (a).

From nominal stress σ_n and nominal strain ε_n, True stress σ_t and true strain ε_t can be obtained from the following equations based on the assumption of constant volume for plastic deformation.

$$\varepsilon\varepsilon_t = \ln(1+\varepsilon\varepsilon_n) \quad (7)$$
$$\sigma_t = \sigma_n(1+\varepsilon\varepsilon_n) \quad (8)$$

Taking ε_{n_m} as the nominal strain ε_n, obtained true stress and strain are denoted as σ_{t_m} and ε_{t_m} respectively, and taking ε_{n_max} as the nominal strain ε_n, obtained true stress and strain are denoted as σ_{t_max} and ε_{t_max}. Thus relations between σ_{t_m} and ε_{t_m} and also σ_{t_max} and ε_{t_max} are shown in Fig. 10 (b). In relation between σ_{t_m} and ε_{t_m} , σ_{t_m} decreases with increase of ε_{t_m} after proof stress and it seems that there is work softening from this relation. In contrary, σ_{t_max} increases with increase of ε_{t_max} and it seems that there is work-hardening from this relation. Conventional nominal strain ε_{n_m} is not the value of strain actually exists on the specimen surface. The maximum strain ε_{n_max} is the strain actually exists on the specimen surface and the relation between σ_{t_max} and ε_{t_max} is the relation actually exists in the specimen. It is found that there exists work-hardening in this material.

Plastic strain $\varepsilon_{p\_}$ can be obtained by subtracting the total strain by the elastic strain as shown in the following equation.

$$\varepsilon\varepsilon_p = \varepsilon\varepsilon_{t\_max} - \sigma_{t\_max}/E \qquad (9)$$

Relation between σ_{t_max} and ε_p in log scale for the data after proof stress is shown in Fig. 11 (a). There is not a linear relationship between them. However, it is clear that gradient of the curve is positive. This gradient expresses work hardening coefficient and it is found that there exists positive work hardening coefficient. Proof stress σ_p is almost 125MPa as shown in Fig. 6 before. The relation between log(σ_{t_max} -σ_p) and log(ε_{pt}) is shown in Fig. 11 (b). From the figure, it is found that there is a linear relation between log(σ_{t_max} -σ_p) and log(ε_p). Thus the following equation holds.

$$\log(\sigma_{t\_max} - \sigma_p) = A + n'\log(\varepsilon\varepsilon_p) \qquad (10)$$

That is

$$\sigma_{t\_max} = \sigma_p + c\varepsilon\varepsilon_p^{\,n'} \qquad (11)$$

where, c=10^A=59.0 and n'=0.673 were obtained from the experimental result. Thus it is found that Ludwik's equation holds for this material.

For steel, SS400 in JIS, the author already published the experimental result (Kato, 2015). From the previous paper, stress-strain relation is shown in Fig. 12 (a). In nominal stress-strain relation shown in Fig. 12 (a), maximum local strain ε_{n_max} differs from the conventional average strain ε_{n_m} after tensile strength due to occurrence of necking by local deformation and in the true stress-strain relation, σ_{t_m} based on the average strain decreases after tensile strength but σ_{t_max} based on the maximum local strain increases after tensile strength. In true stress-strain relation in log scale, the linear relation holds until almost final fracture in σ_{t_max} - ε_{t_max} relation as shown in Fig. 12 (c). Work-hardening coefficient is estimated as n=0.190.

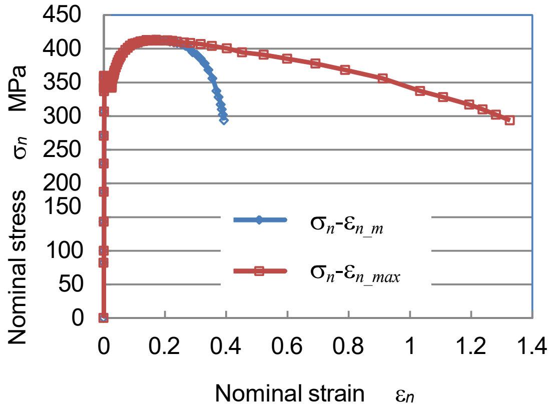

(a) Nominal stress and strain

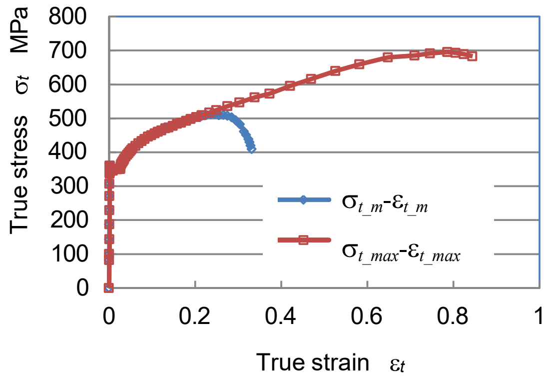

(b) True stress and strain

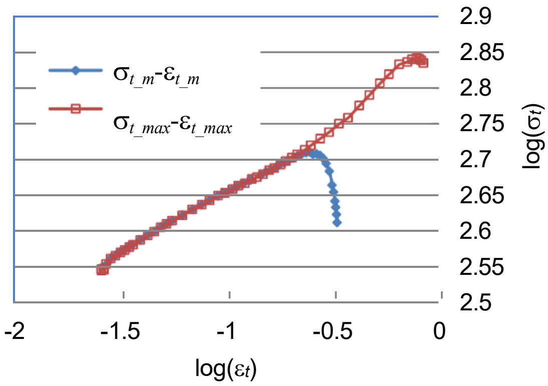

(c) log(σ_t) and log(ε_t)

Fig. 12 Relation between stress and strain (SS400)

From these experiments, in the case that local deformation exists, the conventional average strain in the uniform sectional area takes a value between the maximum local strain and strain at the other location and value of the average strain does not express actual strain appearing in the specimen. The local maximum strain is the strain that actually exists in the specimen. Thus, the local maximum strain should be considered to evaluate stress-strain relation from tensile test in the stage where local deformation occurs. After proof stress for A1050 and after tensile strength for SS400, average strain cannot evaluate true stress-strain relation. We have to take into account the maximum strain in local deformation area to consider stress-strain relation in these cases. For this purpose, measurement of extension in gauge length is not enough and it is necessary to measure strain distribution on material surface during tensile test.

5. Conclusions

While subjecting metals to tensile testing, the author assessed strain distribution using the DIC technique. Thanks to the experiments, we now know these things to be true.

1. Specimens begin to exhibit local plastic strain around the proof stress for the tensile test in A1050.
2. Although work softening was identified in the stress-strain relation for A1050 when evaluating it using standard average strain, work hardening was discovered when considering maximum local strain.

Third, rather than averaging strain across the whole specimen, the greatest strain at a specific location should be considered when assessing the stress-strain relationship in the presence of local deformation.

References

Chu, W.F., Ranson W.F. and Sutton M.A., Application of digital-image-correlation techniques to experimental mechanics, Experimental Mechanics, Vol. **25, No.** 3 (1985), pp. 232-244.

Japanese Industrial Standards Committee, JIS Z2241, (2011).

Kato, A., Measurement of Surface Strain Distribution and Stress-Strain Relation of Steel in Tensile Test, J. of Material Testing Research Association of Japan, Vol. 60, No. 1 (2015), pp. 57-64 (in Japanese).

Kato, A., Measurement of Strain Distribution in Steel Specimen for Tensile Test Using Digital Image Correlation Method, Journal of the Japanese Society for Experimental Mechanics, Vol. **15**- Special Issue (2015), pp. s43-s48.

Noguchi, O., The Properties of Aluminum Sheet for Press Forming, Furukawa-Sky Review, **9**, 3 (2013). pp. 3-10(in Japanese).

Tsuchida, N., Haruo, S., Ohnuki, T. and Tomota, Y., Stress-Strain Curves of Steels, Tetsu-to-Hagane, Vol. **100,** No. 10 (2014), pp. 1191-1206 (in Japanese).

Tokuda, T.. et al, Ductile Fracture in Tension on Notched Plate of Aluminum (A1050P-O), Memoirs of the Yuge National College of Maritime Technology, No. 36 (2014), pp. 46-50 (in Japanese) .